Food Chemistry 181 (2015) 191–197

Contents lists available at ScienceDirect

Food Chemistry

journal homepage: www.elsevier.com/locate/foodchem

Analytical Methods

Preparation of magnetic metal organic frameworks adsorbent modified with mercapto groups for the extraction and analysis of lead in food samples by flame atomic absorption spectrometry

Yang Wang [a,*], Huanhuan Chen [a], Jie Tang [b], Guiqin Ye [a], Huali Ge [a], Xiaoya Hu [a]

[a] Yangzhou University, College of Chemistry and Chemical Engineering, Yangzhou, China
[b] Yangzhou Environmental Monitoring Center Station, Yangzhou, China

ARTICLE INFO

Article history:
Received 20 October 2014
Received in revised form 9 January 2015
Accepted 14 February 2015
Available online 24 February 2015

Keywords:
Magnetic metal organic frameworks
Mercapto groups
Extraction
Lead
Flame atomic absorption spectrometry

ABSTRACT

A novel magnetic metal organic frameworks adsorbent modified with mercapto groups was synthesized and developed for extraction and spectrophotometric determination of trace lead. The adsorbent was characterized by Fourier transforms infrared spectrometer, X-ray diffraction, scanning electron microscopy and vibrating sample magnetometry. The results indicated the adsorbents exhibited high adsorption capacities for lead due to the chelation mechanism between metal cations and mercapto groups. Meanwhile, the lead sorption onto the adsorbents could be easily separated from aqueous solution using a magnetic separation method. Under the optimal conditions, a linear calibration curve in the range from 1 to 20 μg L^{-1} was achieved with an enrichment factor of 100. The limits of detection and quantitation for lead were found to be 0.29 and 0.97 μg L^{-1}, respectively. The developed method was successfully applied to the determination of trace amounts of lead in food samples and certified reference material with satisfactory results.

1. Introduction

Environmental pollution nature of heavy metals and metalloids has received considerable attention. Among these heavy metals, lead is critical for human health. Due to its low excretion rate, lead can accumulate both in the soft tissues and the bones and thus is poisonous to the nervous system and causes brain disorders (Blake et al., 2001; Rodriguez, Bolbot, & Tothill, 2004; Shetty et al., 2003). The intake of lead can occur in human by breathing air, drinking water, and eating food. However, as the levels of lead in food and environmental samples are low, there is a crucial need for the enrichment and preconcentration of trace elements before their analysis (Ferreira et al., 2007; Sitko, Gliwinska, Zawisza, & Feist, 2013).

Solid-phase extraction (SPE) is a widely used approach for sample pretreatment due to its high recovery, short extraction time, high enrichment factor, and ease of automation (Fornieles, Garcia de Torres, Vereda Alonso, & Cano Pavón, 2013; Parham, Pourreza, & Rahbar, 2009; Yang, Liu, Liu, Chen, & Wang, 2012). The choice of appropriate adsorbent is an important factor to obtain good recovery and high enrichment factor in SPE procedure. Recently, numerous adsorbents including activated carbon, SBA-15 silicas, mesoporous manganites and mesoporous titania–silica–phosphonate have been employed as adsorbents in SPE techniques due to their unique large surface areas, well-defined pore sizes, high pore volume and great diversity in surface functionalization (Chouyyok et al., 2010; Lin, Ma, & Yuan, 2011; Liu, Hidajat, Kawi, & Zhao, 2000; Nandi, Sarkar, Seikh, & Bhaumik, 2011). However, the application of such adsorbents often requires post-treatment after adsorption. Sometimes the complete separation and removal of adsorbents from aqueous solutions can be difficult and can cause additional environmental problems. Magnetic solid-phase extraction (MSPE) using magnetic composites as adsorbents are one of the latest developments in SPE techniques. The inherent characteristic of magnetic properties ability has promoted an increasing application of magnetic composites in many fields (Daneshvar Tarigh & Shemirani, 2013; Huo & Yan, 2012; Mashhadizadeh, Amoli-Diva, Shapouri, & Afruzi, 2014). For MSPE, the dispersed magnetic composites can be separated from the matrix quickly in a magnet, and redispersed in the eluent once the external field is removed.

Metal organic frameworks (MOFs), forming by the coordination of a metallic center and an organic ligand, have proved to be a new class of materials. The high porosity and specific surface of MOFs has directed their potential applications toward catalysis, sensors, separation, and drug delivery (Dhakshinamoorthy, Alvaro, &

* Corresponding author. Tel/fax: +86 51487975587.
E-mail address: wangyzu@126.com (Y. Wang).

http://dx.doi.org/10.1016/j.foodchem.2015.02.080
0308-8146/

Garcia, 2011; Huxford, Rocca, & Lin, 2010; Petit, Levasseur, Mendoza, & Bandosz, 2012; Yu et al., 2014). Moreover, MOFs also show great promise in the analytical applications such as the capture of heavy metal ions by the chelation coordination effect between metal ions and functional group in the linker (Fang et al., 2010; He et al., 2013; Yang et al., 2013). However, the use of functional linkers is limited by the conventional solvothermal procedure of MOFs. Postsynthetic modification has been utilized as a powerful tool for introducing functionality to MOFs by covalent reactions. The incorporation of functional groups on the linking ligands can provide an opportunity to develop MOFs with a variety of functionalities (Bernt, Guillerm, Serre, & Stock, 2011; Gadzikwa et al., 2008; Jung et al., 2011).

Herein, we report the preparation of mercapto groups modified magnetic metal organic frameworks (SH-Fe_3O_4/$Cu_3(BTC)_2$) adsorbents and the potential application for the extraction of trace heavy metal ions followed by flame atomic absorption spectroscopy (FAAS). The adsorbent possesses large a surface area because of the nanometer size. The superparamagnetic Fe_3O_4 contributes to the rapid separation of the adsorbent from the matrix solution. Mercapto groups provide more bonding sites for heavy metals. Based on these considerations, extracting trace heavy metals from water solutions can be readily achieved. To the best of our knowledge, no research on the application of SH-Fe_3O_4/$Cu_3(BTC)_2$ composites for extraction and determination of trace lead in food samples and certified reference material has been reported.

2. Experimental

2.1. Reagents and materials

Copper nitrate, ferrous chloride, ferric chloride, 1,3,5-benzene tricarboxylic acid (H_3BTC, 98%), dithioglycol, anhydrous ethanol, dimethylformamide (DMF), sodium hydroxide, hydrogen peroxide, lead nitrate, ammonium hydroxide, perchloric acid and nitric acid were of analytical reagent grade and purchased from Sinopharm Chemical Reagent Co., Ltd. (Shanghai, China). The lead stock solution of 1000 mg L^{-1} was prepared by dissolving 33.12 g of $Pb(NO_3)_2$ in 100 mL deionized water. Working standard solutions of lead were prepared by stepwise dilution of the stock solution with deionized water. Reference materials GBW10017 (Milk powder) was purchased from the BHH Biotechnology Co., Ltd (Beijing, China). Rice, pig liver and tea leaves were purchased from the local market. Water sample was collected from the laboratory. Double deionized water (18 MΩ cm) was used throughout the experiments.

2.2. Apparatus

The FTIR spectra were collected using a Cary 610/670 infrared microspectrometer (America Varian). The powder X-ray diffraction (XRD) patterns were collected with a D8 Advance X-ray diffractometer (Bruker Co., Germany) from 5° to 50°. The morphology of the composites was recorded by Hitachi S-4800 microscope (Japan) with ethanol spitting and then sonicated for 30 min. The magnetic property was analyzed by using a vibrating sample magnetometer (VSM, LDJ9600). An atomic absorption spectrometer (AEEnit 700) with flame was used for testing lead and the instrumental parameters were adjusted according to the manufacturer recommendations. A continuous flow atomic fluorescence spectrometer (AFS-3100) was employed for the method validation. For atomic fluorescence spectrometer, the sample solutions were analyzed under the following conditions: lamp current (30 mA), atomizer height (8 mm), negative high voltage of the PTM (300 V), flow rate of carrier gas (400 mL min^{-1}), flow rate of shield gas (900 mL min^{-1}), injection volume (1 mL), read mode (peak area). A permanent magnet was used for the isolation of the analytes from the complicated matrix.

2.3. Synthesis of Fe_3O_4

The magnetic nanoparticles were prepared according to the previous report with small modifications (Kang, Risbud, Rabolt, & Stroeve, 1996). 10.8 g $FeCl_3{\cdot}6H_2O$ and 4.2 g $FeCl_2{\cdot}4H_2O$ were completely dissolved in 25 mL of HCl (6 mol L^{-1}). Then 50 mL NH_4OH (25% wt) was quickly added to the above aqueous solutions at 60 °C for 30 min. After cooling to ambient temperature, the black precipitation was separated by a magnet and further washed with distilled water and dried at 60 °C for 6 h. N_2 was used as the protective gas throughout the experiment.

2.4. Synthesis of Fe_3O_4/$Cu_3(BTC)_2$

1.0 g H_3BTC dissolved in 80 mL mixture solutions (DMF: anhydrous ethanol = 1:1) was transferred into a 250 mL flask. Under magnetic stirring, 0.15 g Fe_3O_4 dissolved in 20 mL anhydrous ethanol was added and refluxed for a while at 70 °C. Afterwards, 2.0 g $Cu(NO_3)_2{\cdot}3H_2O$ dissolved in 40 mL deionized water was slowly added to the above solution and this was refluxed for 4 h. After cooling to ambient temperature, the product was filtered off, washed several times with deionized water (50 mL) and ethanol (10 mL), and then dried at 120 °C for 10 h.

2.5. Synthesis of SH-Fe_3O_4/$Cu_3(BTC)_2$

0.11 g prepared Fe_3O_4/$Cu_3(BTC)_2$ sample was dried at 150 °C for 12 h, and then suspended in 10 mL anhydrous toluene. 0.6 mL dithioglycol solution (0.24 mol L^{-1}) was added into the mixture solution and stirred 24 h. Finally, the blue-green powder was collected by filtration, washed with 15 mL ethanol five times, and dried 24 h at room temperature.

2.6. Sample preparation

(1) 10 g of rice sample was triturated and homogenized. Then a portion of 3.0 g was dried in an oven at 110 °C to constant weight. The dried sample was placed in a furnace and heated to 450 °C, and concentrated nitric acid was added dropwise until white ashes appeared. After that, the sample was dissolved in 1 mL 1 mol L^{-1} nitric acid and diluted to 10 mL with deionized water. (2) Pig livers were heated in an oven at 80 °C for 3 h. After drying, 1.0 g sample was dissolved 5 mL of nitric acid and transferred into a digestion tube at room temperature overnight. Then the tube was heated at 160 °C until the contents nearly dried. After cooling, 2 mL perchloric acid was added, and the contents were further heated to dryness at 210 °C. Finally the residue was dissolved with 10 mL deionized water when the tube was cooled down. (3) Water sample was filtered using a 0.45 μm filter prior to analysis. (4) 1.0 g of tea leaves was added in a solution including 5 mL of concentrated HNO_3 and 2 mL of 30% H_2O_2. Then the mixture was transferred into a 10 mL flask, and heated 200 °C for 20 min. After cooling to the room temperature, the samples were transferred to a 50 mL volumetric flask and diluted to the mark. (5) 1.0 g certified reference material GBW10017 (milk powder) was carbonized in 10 mL concentrated H_2SO_4 with another 10 min heating. After cooling, the sample was dissolved in 15 mL 1 mol L^{-1} HNO_3 and diluted to 100 mL with deionized water.

2.7. Extraction process

The magnetic solid-phase extraction procedure was described as follows: 10 mg of prepared SH-Fe_3O_4/$Cu_3(BTC)_2$ adsorbent was added to 10 mL of spiked sample solution adjusted at pH 6 using 1 mol L^{-1} sodium hydroxide or 1 mol L^{-1} nitric acid. The solution was stirred for 15 min to facilitate the adsorption of lead on to the surface of SH-Fe_3O_4/$Cu_3(BTC)_2$. The magnetic sorbent was collected using an external magnet and supernatant water was decanted. Finally, the extracted analyte was desorbed with 2.0 mL HNO_3 and injected into the FAAS for analysis.

3. Results and discussion

3.1. Characterization of the SH-Fe_3O_4/$Cu_3(BTC)_2$ composites

Fig. 1 shows the FTIR spectrum of $Cu_3(BTC)_2$, Fe_3O_4/$Cu_3(BTC)_2$, and SH-Fe_3O_4/$Cu_3(BTC)_2$. In FTIR of $Cu_3(BTC)_2$, the peaks appearing at 1374 cm^{-1} and 1449 cm^{-1} are attributed to the stretching vibration absorption peak of the C=C bonds of the benzene ring, meanwhile the peak at 3238 cm^{-1} is due to the stretching vibration of the C–H bond in the benzene ring. The peaks at 1646 cm^{-1} could be related to the stretching vibration absorption peak of the C=O bonds and the peak at 730 cm^{-1} was the stretching vibration absorption peak of the Cu–O bonds. From the FTIR spectrum of Fe_3O_4/$Cu_3(BTC)_2$, the primary stretching vibration peak of Fe–O at 590 cm^{-1} is not very obvious due to the low content of Fe_3O_4 (Peng et al., 2012). The peak at 851 cm^{-1} in the spectrum of SH-Fe_3O_4/$Cu_3(BTC)_2$ is the characteristic S–C stretching vibration peak (Wang, Xie, Wu, Ge, & Hu, 2013), indicating that dithioglycol were coated onto Fe_3O_4/$Cu_3(BTC)_2$ successfully.

The synthesized material phase purity and crystal structure were characterized by powder XRD pattern (Fig. 2). The main diffraction peaks of $Cu_3(BTC)_2$ are 7.37°, 9.50°, 11.6°, 13.41°, 17.46°, 19.03° and 25.93°, and these values are corresponding to the previous work (Kumar, Kumar, & Kulandainathan, 2012). Fig. 2b shows that the presence of Fe_3O_4 does not change the main diffraction peaks of $Cu_3(BTC)_2$, but the primary peak of Fe_3O_4 around 35° cannot be observed, probably because the content of Fe_3O_4 is very low and the peak was covered by the $Cu_3(BTC)_2$ peak (Yu, Gou, Zhou, Bao, & Gu, 2011). When the Fe_3O_4/$Cu_3(BTC)_2$ was coated with dithioglycol, the sketch of $Cu_3(BTC)_2$ crystal is well retained, but the peak strength is weakened obviously. This may be due to the interaction between –SH and Cu^{2+}, leading to a decline in crystallinity of $Cu_3(BTC)_2$.

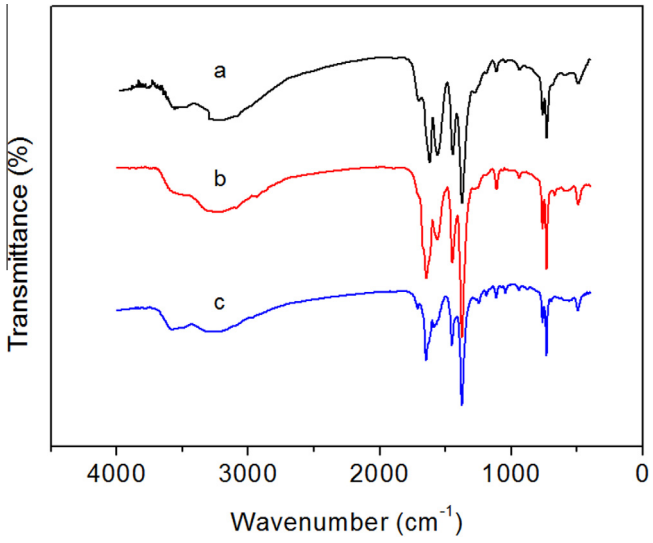

Fig. 1. FTIR spectra of as-synthesized $Cu_3(BTC)_2$ (a), Fe_3O_4/$Cu_3(BTC)_2$ (b), and SH-Fe_3O_4/$Cu_3(BTC)_2$ (c).

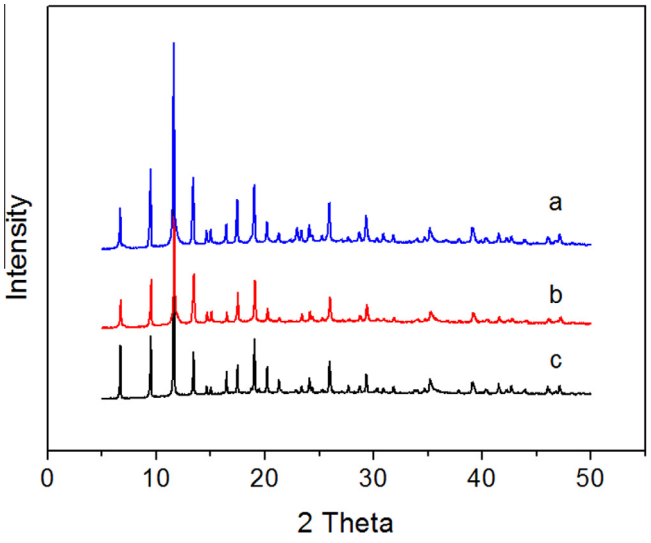

Fig. 2. XRD patterns of as-synthesized $Cu_3(BTC)_2$ (a), Fe_3O_4/$Cu_3(BTC)_2$ (b), and SH-Fe_3O_4/$Cu_3(BTC)_2$ (c).

Fig. 3 shows the SEM images of $Cu_3(BTC)_2$, Fe_3O_4/$Cu_3(BTC)_2$, and SH-Fe_3O_4/$Cu_3(BTC)_2$. As shown in Fig. 3a, a regularly octahedral morphology crystals of synthesized $Cu_3(BTC)_2$ were obtained and its average size is about 11 μm. After adding Fe_3O_4, the crystal of Fe_3O_4/$Cu_3(BTC)_2$ decreased and surface became more rougher. But we can observed that the adding of Fe_3O_4 does not change the octahedral morphology of $Cu_3(BTC)_2$. Compared with $Cu_3(BTC)_2$, the crystal surface and form of SH-Fe_3O_4/$Cu_3(BTC)_2$ have changed greatly. The reason is probably due to the fact that $Cu_3(BTC)_2$ lost structural water at 150 °C in the process of preparation (Wang et al., 2013).

The magnetic properties of Fe_3O_4/$Cu_3(BTC)_2$ and SH-Fe_3O_4/$Cu_3(BTC)_2$ were determined by vibrating sample magnetometer (VSM) at normal temperature. The saturation magnetization value of Fe_3O_4/$Cu_3(BTC)_2$ was 7.96 emu g^{-1}. After adding dithioglycol, the value decreased to 4.59 emu g^{-1}. However, the magnetic susceptibility of SH-Fe_3O_4/$Cu_3(BTC)_2$ is large enough to facilitate the quick separation of composites from solution using a regular magnet.

3.2. Optimization of the MSPE conditions

The pH value of the solution was an important parameter influencing the adsorption process of metal ions on the sorbent because of the protonation or deprotonation reaction to the sorbent and the hydrolysis reaction to the metal ions in the alkaline condition. Therefore, solution pH is the first parameter to be optimized on the adsorption of lead by the SH-Fe_3O_4/$Cu_3(BTC)_2$ with a lead concentration of 10 μg L^{-1} (Fig. 4a). It was found that the signal intensity increased with increasing solution pH and then remained nearly constant from 3 to 7. This could be due to the reason that lead species might be changed in the adsorption process with the pH value of the solution varied. From the pH dependence, different species of lead, such as Pb^{2+}, $PbOH^+$, and $Pb(OH)_2$ existed with pH value varied. The corresponding complexation reactions among different lead species with mercapto groups can be expressed as follows:

$$-SH + Pb^{2+} \rightarrow -S-Pb^{+} + H^{+} \quad (1)$$

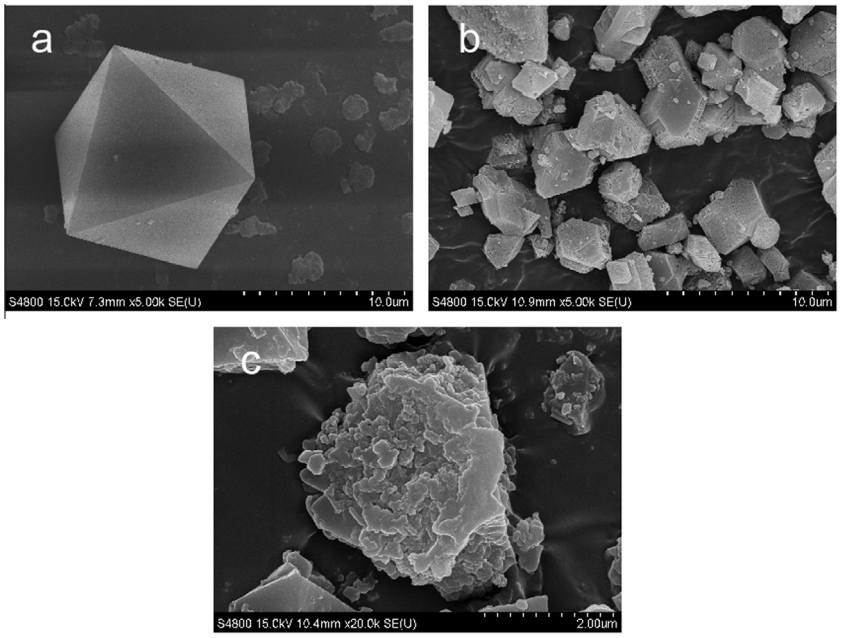

Fig. 3. SEM images of as-synthesized $Cu_3(BTC)_2$ (a), $Fe_3O_4/Cu_3(BTC)_2$ (b), and SH-$Fe_3O_4/Cu_3(BTC)_2$ (c).

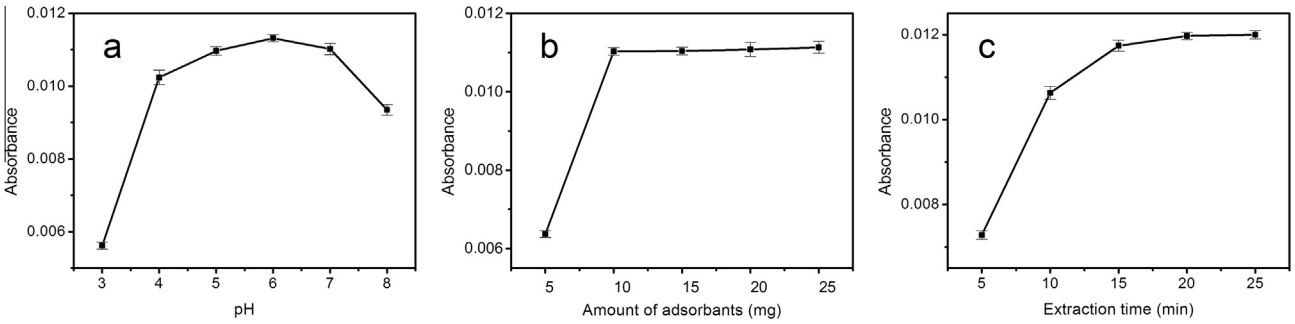

Fig. 4. Effects of sample pH (a), amount of adsorbents (b), and extraction time (c) on the lead adsorption.

$$-SH + PbOH^+ \rightarrow -S-PbOH + H^+ \quad (2)$$

$$-SH + Pb(OH)_2 \rightarrow -S-PbOH + H_2O \quad (3)$$

At low pH value, the dominant species of lead in the solution was Pb^{2+}. Although competitive adsorption of Pb^{2+} and hydrogen ions at low pH exists, the affinity between Pb^{2+} and mercapto groups was higher than that between hydrogen ions and mercapto groups. Lead complexation to mercapto groups on the SH-Fe_3O_4/$Cu_3(BTC)_2$ led to a positive charge $-S-Pb^+$. Electrostatic repulsion between the Pb^{2+} ions and the $-S-Pb^+$ complexes surface increased. These effects resulted in the reduction of Pb^{2+} ions adsorption on the SH-$Fe_3O_4/Cu_3(BTC)_2$ composites. As pH increasing, pH above 3, the reaction of the hydroxylated lead form resulted in the formation of a neutral complexed form ($-S-Pb(OH)$). Thus, no electrostatic repulsion was expected to occur and leading the adsorption capacity of lead reaching a plateau value in the pH range of 3–6. When pH > 7, the signal intensity began to decrease due to the formation of white $Pb(OH)_2$ precipitate (Wu, Li, Xu, Wei, & Li, 2010). Therefore, the optimum pH value of 6 was selected in further experiments.

An optimum adsorbent amount is essentially required to maximize the interactions between metal ions and adsorption sites of adsorbent in the solution. To evaluate the optimum amount of SH-$Fe_3O_4/Cu_3(BTC)_2$ composites, 5, 10, 15, 20, and 25 mg of SH-$Fe_3O_4/Cu_3(BTC)_2$ composites were added to 10 mL of aqueous solution containing 10 μg L^{-1} lead, respectively. Fig. 4b indicated that 10 mg adsorbent was enough to achieve a satisfactory result because of the large surface area and high adsorption efficiency of SH-$Fe_3O_4/Cu_3(BTC)_2$ composites. According to the above consequence, the optimal amount of the absorbent was adjusted to 10 mg.

A certain extraction time is required after the adsorbents are dispersed into the solution in order to facilitate the interaction between analyte and SH-$Fe_3O_4/Cu_3(BTC)_2$ composites. The extraction time was studied by varying the mixing time of SH-Fe_3O_4/$Cu_3(BTC)_2$ composites-sample solutions ranging from 5 to 25 min. As shown in Fig. 4c, the signal intensity of lead increased significantly with an extending time from 5 to 15 min. Once adjusted from 15 to 25 min, adsorption amounts had no remarkable improvement. It may be due to the fact that the distribution equilibrium between the analytes and adsorbents was easily achieved in only 15 min due to the strong complexation interactions, and a prolonged time did not contribute more enhancement of enrichment efficiency. Hence, the best extraction time of 15 min was employed as the optimum condition in this work.

In order to obtain a higher enrichment factor, a larger volume of sample solution is required. The effect of sample solution volume on the extraction of lead was studied by using different volumes (10–400 mL) of aqueous solution spiked with a fixed 10 μg L^{-1} of

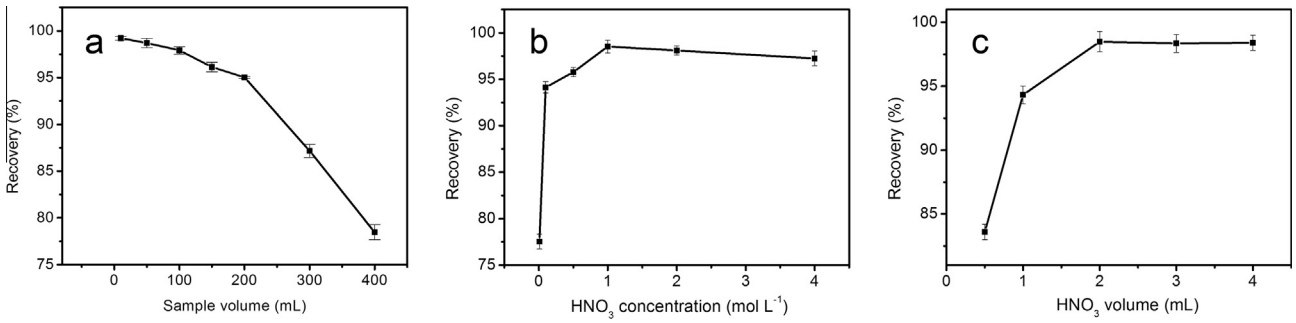

Fig. 5. Effects of sample volume (a), eluent concentration (b), and eluent volume (c) on the lead adsorption.

Table 1
Comparison of the present method with other systems fort the determination of lead.

Sorbent	Detector	Linear range ($\mu g\ L^{-1}$)	LOD ($\mu g\ L^{-1}$)	RSD (%)	Adsorption capacity ($mg\ g^{-1}$)	References
Triazine/Fe_3O_4 nanoparticles	FAAS	3.0–100	0.7	1.3	134.9	Behzad, Balati, Amini, and Ghanbari (2014)
Magnetic multi-wall carbon nanotube	FAAS	5–200	1.0	4.3	–	Daneshvar Tarigh and Shemirani (2013)
1-(2-pyridylazo)-2-naphtol-Fe_3O_4/TiO_2	FAAS	4–470	1.21	2.2	11.18	Fasih Ramandi and Shemirani (2015)
Solid Sulfur	FAAS	10–300	3.2	5.1	15.6	Parham et al. (2009)
Ag12 cuboctahedral node	FAAS	2–180	0.5	4	120	Salarian, Ghanbarpour, Behbahani, Bagheri, and Bagheri (2014)
Fe_3O_4-pyridine/$Cu_3(BTC)_2$	FAAS	2.5–125	1.1	4.5	190	Sohrabi, Matbouie, Asgharinezhad, and Dehghani (2013)
Graphene	FAAS	10.0–600	0.61	3.25	16.6	Wang, Gao, Zang, Li, and Ma (2012)
SH-Fe_3O_4/$Cu_3(BTC)_2$	FAAS	1.0–20	0.29	2.4	198	This work

lead in the optimal conditions (Fig. 5a). The extraction, that is the percent extraction of lead, is calculated from the following equation:

$$\text{extraction}\% = (C_A - C_B)/C_A \times 100 \quad (4)$$

where C_A and C_B are the concentrations of the lead ions in the solution before and after extraction, respectively. The experimental results demonstrated that the extraction was quantitative (recovery > 95%) with the sample volumes up to 200 mL, and a decrease was observed with further increase in sample volume. With an elution volume of 2.0 mL, a theoretical enrichment factor of 100 was achieved by this method. However, for convenience, all the experiments were carried out with 10 mL of the aqueous phase.

Various desorbing reagents were used to find the best desorbing solution for the adsorbed metal ions. From the pH study, it has been found that the adsorption of lead on SH-Fe_3O_4/$Cu_3(BTC)_2$ composites was negligible at low pH. This suggested that desorption of lead from SH-Fe_3O_4/$Cu_3(BTC)_2$ composites was possible at lower acid environment. Therefore, HNO_3 solutions of different concentration (0.01, 0.1, 0.5, 1, 2, and 4 mol L^{-1}) were used to examine the desorption study. As shown in Fig. 5b, 1 mol L^{-1} of HNO_3 provided an effective elution of lead from SH-Fe_3O_4/$Cu_3(BTC)_2$ composites. The higher desorption efficiency at lower pH value could be referred to the sufficiently high hydrogen ion concentration, which led to the strong competitive adsorption. Therefore, 1 mol L^{-1} of HNO_3 was chosen as an eluent for the metal ions from SH-Fe_3O_4/$Cu_3(BTC)_2$ composites. The effect of eluent volume in the range of 0.5–4 mL on the recovery of the lead was given in Fig. 5c. The results indicated that quantitative recovery could be obtained with 2 mL of HNO_3 (1 mol L^{-1}). Therefore, volume of 2.0 mL of eluent for desorption of lead was used in the further experiments.

The capacity of the adsorbent is an important factor because it determines how much adsorbent is required to quantitatively remove a specific amount of metal ions from the solutions. In order to determinate the adsorption capacity, 10 mg of SH-Fe_3O_4/$Cu_3(BTC)_2$ composites and 10 mL of various concentrations of lead was equilibrated for 15 min. The amount of lead adsorbed per unit mass of the adsorbent increased with the initial concentration, and the static adsorption capacity of SH-Fe_3O_4/$Cu_3(BTC)_2$ composites was found to be 198 mg g^{-1} for lead.

3.3. The effects of coexisting ions

There are several ions in the food sample, such as Na^+, K^+, Cl^-, Fe^{3+}, Cu^{2+}, Mg^{2+}, Zn^{2+}, and Ca^{2+}. In order to demonstrate the selectivity of the developed method, various metal ions were added to 10 mL aqueous solutions containing 10 $\mu g\ L^{-1}$ lead. The tolerance limit was taken as the concentration of the interfering ions causing a variation in the intensity of lead within ±5%. The tolerable ratio of each species concentration was as follows: 2000-fold for Na^+, K^+, Cl^-, Fe^{3+}, Cu^{2+}, Al^{3+}, Mn^{2+}, NO_3^-, NH_4^+ and PO_4^{3-}; 1000-fold for Mg^{2+}, Zn^{2+} and Ca^{2+}; 500-fold for Co^{2+}, Ni^{2+}, As^{3+} and SO_4^{2-}. Cd^{2+} will cause interference if its concentration is more than 100 times over the lead. From the tolerance data, it can be observed that the potentially interfering ions have no significant effects on preconcentration of lead by the proposed sample pretreatment technique.

3.4. Analytical figures of merit and method validation

Under the optimized conditions, calibration curve was constructed for the determination of lead according to the general procedure. Five standard solutions were used to obtain the calibration curve, and linearity was maintained 1–20 $\mu g\ L^{-1}$ for the lead in the initial solution. The correlation of determination (R^2) was 0.9975. The limits of detection, defined as LOD = $3\sigma/s$, where σ is the standard deviation of 11 replicate blank signals and s is the slope of the calibration curve after preconcentration, for a sample volume of

Table 2
Analytical results for food samples (mean ± standard deviation, $n = 6$).

Sample	Original ($\mu g\ L^{-1}$)	Spiked ($\mu g\ L^{-1}$)	Found ($\mu g\ L^{-1}$)	AFS ($\mu g\ L^{-1}$)	Recovery (%)
Rice	8.54 ± 0.03	2.00	10.61 ± 0.03	10.57 ± 0.05	103.5
		5.00	13.52 ± 0.04	13.49 ± 0.03	99.6
Pig liver	10.01 ± 0.05	2.00	12.03 ± 0.02	11.98 ± 0.04	101.0
		5.00	14.95 ± 0.06	15.01 ± 0.01	98.8
Tea leaves	14.65 ± 0.02	2.00	16.68 ± 0.05	16.67 ± 0.02	101.5
		5.00	19.50 ± 0.03	19.41 ± 0.08	97.0
Water	1.32 ± 0.17	1.00	2.34 ± 0.05	2.42 ± 0.06	102.0
		2.00	3.31 ± 0.07	3.38 ± 0.03	99.5

10 mL, was found to be 0.29 $\mu g\ L^{-1}$. While the limit of quantification, defined as LOD = $10\sigma/s$, was found to be 0.97 $\mu g\ L^{-1}$. The relative standard deviation for 6 separate experiments for the determination of 1.0, 10, and 15 $\mu g\ L^{-1}$ of lead was 2.4%, 1.8%, and 1.7%, respectively. Moreover, it was found that the prepared SH-Fe_3O_4/$Cu_3(BTC)_2$ composites were relatively stable up to at least 5 adsorption-elution cycles without any obvious decrease in recovery. The comparison results of the proposed method with some reported procedures for the determination of lead are given in Table 1. Due to the high surface area of metal organic frameworks and the presence of the free mercapto groups, the adsorbents exhibit a high adsorption capacity and a low detection limit than other materials. In addition, the separation of lead adsorbed magnetic metal organic frameworks from the solution can easily be achieved via an external magnetic field. These advantages open up new avenues for the preparation and application of functionalized magnetic MOF through postsynthetic modification strategies as a future sample pretreatment technique. In order to evaluate the validity of the proposed procedure, the method was applied to the determination of the content of lead in different food samples (rice, pig liver, water, and tea leaves). After digestion, the sample was determined directly or with an appropriate dilution to draw the lead concentration within the linear range. The accuracy of the method was verified by the analysis of samples spiked with known amounts of lead with detection by flame absorption spectrometry. As could be shown in Table 2, recoveries for the target analytes ranged from 97.0% to 103.5%. The contents of lead determined in rice, pig liver, tea leaves, and water were 0.085, 0.100, 0.732, and 0.001 mg kg^{-1}, respectively. The results of the present work were also compared with those obtained with the hydride generation atomic fluorescence spectrometry, and there was no significant difference between the values of both analytical methods. In addition, one certified reference material GBW10017 (milk powder) was further used to evaluate the accuracy for lead determination. It was found that the obtained content of lead ($0.077 \pm 0.013\ \mu g\ g^{-1}$) was in keeping with the certified value ($0.07 \pm 0.02\ \mu g\ g^{-1}$). The results indicated that the proposed method can be reliably used for the determination of lead in food samples.

4. Conclusions

The proposed method demonstrated great potentials of SH-Fe_3O_4/$Cu_3(BTC)_2$ composites as an appropriate adsorbent in MSPE for the determination of trace lead in food samples. The presence of thiol groups and high surface area of $Cu_3(BTC)_2$ composites significantly enhanced the sensitivities and adsorption capacity of lead. SH-Fe_3O_4/$Cu_3(BTC)_2$ composites with adsorbed heavy metal ions can be simply collected from samples with magnetic separations by an external magnetic field, and the adsorbed lead was ready to be desorbed with HNO_3 solution followed by FAAS analysis. The developed method is rapid and sensitive and is promising for routine analysis of trace lead in food materials.

Acknowledgements

This work was supported by the National Natural Science Foundation of China (21205103, 21275124), Jiangsu Provincial Nature Foundation of China (BK2012258), the Key Laboratory Foundation of Environmental Material and Engineering of Jiangsu Province (K13077) and a Project Funded by the Priority Academic Program Development of Jiangsu Higher Education Institutions.

References

Behzad, S. K., Balati, A., Amini, M. M., & Ghanbari, M. (2014). Triazine-modified magnetite nanoparticles as a novel sorbent for preconcentration of lead and cadmium ions. *Microchimica Acta, 181*, 1781–1788.
Bernt, S., Guillerm, V., Serre, C., & Stock, N. (2011). Direct covalent post-synthetic chemical modification of Cr-MIL-101 using nitrating acid. *Chemical Communications, 47*, 2838–2840.
Blake, D. A., Jones, R. M., Blake, R. C., II, Pavlov, A. R., Darwish, I. A., & Yu, H. N. (2001). Antibody-based sensors for heavy metal ions. *Biosensors & Bioelectronics, 16*, 799–809.
Chouyyok, W., Shin, Y., Davidson, J., Samuels, W. D., Lafemina, N. H., Rutledge, R. D., et al. (2010). Selective removal of copper(II) from natural waters by nanoporous sorbents functionalized with chelating diamines. *Environmental Science & Technology, 44*, 6390–6395.
Daneshvar Tarigh, G., & Shemirani, F. (2013). Magnetic multi-wall carbon nanotube nanocomposite as an adsorbent for preconcentration and determination of lead (II) and manganese (II) in various matrices. *Talanta, 115*, 744–750.
Dhakshinamoorthy, A., Alvaro, M., & Garcia, H. (2011). Aerobic oxidation of styrenes catalyzed by an iron metal organic framework. *ACS Catalysis, 1*, 836–840.
Fang, Q. R., Yuan, D. Q., Sculley, J., Li, J. R., Han, Z. B., & Zhou, H. C. (2010). Functional mesoporous metal-organic frameworks for the capture of heavy metal ions and size-selective catalysis. *Inorganic Chemistry, 49*, 11637–11642.
Fasih Ramandi, N., & Shemirani, F. (2015). Selective ionic liquid ferrofluid based dispersive-solid phase extraction for simultaneous preconcentration/separation of lead and cadmium in milk and biological samples. *Talanta, 131*, 404–411.
Ferreira, S. L. C., de Andrade, J. B., Korn, M. das G. A., Pereira, M. de G., Lemos, V. A., dos Santos, W. N. L., et al. (2007). Review of procedures involving separation and preconcentration for the determination of cadmium using spectrometric techniques. *Journal of Hazardous Materials, 145*, 358–367.
Fornieles, A. C., Garcia de Torres, A., Vereda Alonso, E. I., & Cano Pavón, J. M. C. (2013). Determination of antimony, bismuth and tin in natural waters by flow injection solid phase extraction coupled with online hydride generation inductively coupled plasma mass spectrometry. *Journal of Analytical Atomic Spectrometry, 28*, 364–372.
Gadzikwa, T., Lu, G., Stern, C. L., Wilson, S. R., Hupp, J. T., & Nguyen, S. T. (2008). Covalent surface modification of a metal-organic framework: selective surface engineering via Cu^{I}-catalyzed Huisgen cycloaddition. *Chemical Communications, 43*, 5493–5495.
He, J., Zha, M., Cui, J., Zeller, M., Hunter, A. D., Yiu, S. M., et al. (2013). Convenient detection of Pd(II) by a metal-organic framework with sulfur and olefin functions. *Journal of the American Chemical Society, 135*, 7807–7810.
Huo, S. H., & Yan, X. P. (2012). Facile magnetization of metal-organic framework MIL-101 for magnetic solid-phase extraction of polycyclic aromatic hydrocarbons in environmental water samples. *Analyst, 137*, 3445–3451.
Huxford, R. C., Rocca, J. D., & Lin, W. (2010). Metal-organic frameworks as potential drug carriers. *Current Opinion in Chemical Biology, 14*, 262–268.
Jung, S., Kim, Y., Kim, S. J., Kwon, T. H., Huh, S., & Park, S. (2011). Bio-functionalization of metal-organic frameworks by covalent protein conjugation. *Chemical Communications, 47*, 2904–2906.
Kang, Y. S., Risbud, S., Rabolt, J. F., & Stroeve, P. (1996). Synthesis and characterization of nanometer-size Fe_3O_4 and γ-Fe_2O_3 particles. *Chemistry of Materials, 8*, 2209–2211.
Kumar, R. S., Kumar, S. S., & Kulandainathan, M. A. (2012). Highly selective electrochemical reduction of carbon dioxide using Cu based metal organic framework as an electrocatalyst. *Electrochemistry Communications, 25*, 70–73.

Lin, X. Z., Ma, T. Y., & Yuan, Z. Y. (2011). Titania–silica–phosphonate triconstituent hybrid mesoporous materials as adsorbents in gas and liquid phases. *Chemical Engineering Journal, 166*, 1144–1151.

Liu, A. M., Hidajat, K., Kawi, S., & Zhao, D. Y. (2000). A new class of hybrid mesoporous materials with functionalized organic monolayers for selective adsorption of heavy metal ions. *Chemical Communications, 13*, 1145–1146.

Mashhadizadeh, M. H., Amoli-Diva, M., Shapouri, M. R., & Afruzi, H. (2014). Solid phase extraction of trace amounts of silver, cadmium, copper, mercury, and lead in various food samples based on ethylene glycol bis-mercaptoacetate modified 3-(trimethoxysilyl)-1-propane thiol coated Fe_3O_4 nanoparticles. *Food Chemistry, 151*, 300–305.

Nandi, M., Sarkar, K., Seikh, M., & Bhaumik, A. (2011). Mesoporous lanthanum-manganese oxides with nanoscale periodicity, high surface area and ferromagnetic property. *Microporous and Mesoporous Materials, 143*, 392–397.

Parham, H., Pourreza, N., & Rahbar, N. (2009). Solid phase extraction of lead and cadmium using solid sulfur as a new metal extractor prior to determination by flame atomic absorption spectrometry. *Journal of Hazardous Materials, 163*, 588–592.

Peng, L., Qin, P., Lei, M., Zeng, Q. R., Song, H., Yang, J., et al. (2012). Modifying Fe_3O_4 nanoparticles with humic acid for removal of rhodamine B in water. *Journal of Hazardous Materials, 209–210*, 193–198.

Petit, C., Levasseur, B., Mendoza, B., & Bandosz, T. J. (2012). Reactive adsorption of acidic gases on MOF/graphite oxide composites. *Microporous and Mesoporous Materials, 154*, 107–112.

Rodriguez, B. B., Bolbot, J. A., & Tothill, I. E. (2004). Development of urease and glutamic dehydrogenase amperometric assay for heavy metals screening in polluted samples. *Biosensors & Bioelectronics, 19*, 1157–1167.

Salarian, M., Ghanbarpour, A., Behbahani, M., Bagheri, S., & Bagheri, A. (2014). A metal-organic framework sustained by a nanosized Ag12 cuboctahedral node for solid-phase extraction of ultra traces of lead(II) ions. *Microchimica Acta, 181*, 999–1007.

Shetty, R. S., Deo, S. K., Shah, P., Sun, Y., Rosen, B. P., & Daunert, S. (2003). Luminescence-based whole-cell-sensing systems for cadmium and lead using genetically engineered bacteria. *Analytical and Bioanalytical Chemistry, 376*, 11–17.

Sitko, R., Gliwinska, B., Zawisza, B., & Feist, B. (2013). Ultrasound-assisted solid-phase extraction using multiwalled carbon nanotubes for determination of cadmium by flame atomic absorption spectrometry. *Journal of Analytical Atomic Spectrometry, 28*, 405–410.

Sohrabi, M. R., Matbouie, Z., Asgharinezhad, A. A., & Dehghani, A. (2013). Solid phase extraction of Cd(II) and Pb(II) using a magnetic metal-organic framework, and their determination by FAAS. *Microchimica Acta, 180*, 589–597.

Wang, Y., Gao, S., Zang, X., Li, J., & Ma, J. (2012). Graphene-based solid-phase extraction combined with flame atomic absorption spectrometry for a sensitive determination of trace amounts of lead in environmental water and vegetable samples. *Analytica Chimica Acta, 716*, 112–118.

Wang, Y., Xie, J., Wu, Y. C., Ge, H. L., & Hu, X. Y. (2013). Preparation of a functionalized magnetic metal-organic framework sorbent for the extraction of lead prior to electrothermal atomic absorption spectrometer analysis. *Journal of Materials Chemistry A, 1*, 8782–8789.

Wu, S. J., Li, F. T., Xu, R., Wei, S. H., & Li, G. T. (2010). Synthesis of thiol-functionalized MCM-41 mesoporous silicas and its application in Cu(II), Pb(II), Ag(I), and Cr(III) removal. *Journal of Nanoparticle Research, 12*, 2111–2124.

Yang, G. S., Lang, Z. L., Zang, H. Y., Lan, Y. Q., He, W. W., Zhao, X. L., et al. (2013). Control of interpenetration in S-containing metal-organic frameworks for selective separation of transition metal ions. *Chemical Communications, 49*, 1088–1090.

Yang, T., Liu, L. H., Liu, J. W., Chen, M. L., & Wang, J. H. (2012). Cyanobacterium metallothionein decorated graphene oxide nanosheets for highly selective adsorption of ultra-trace cadmium. *Journal of Materials Chemistry, 22*, 21909–21916.

Yu, C. M., Gou, L. L., Zhou, X. H., Bao, N., & Gu, H. Y. (2011). Chitosan-Fe_3O_4 nanocomposite based electrochemical sensors for the determination of bisphenol A. *Electrochimica Acta, 56*, 9056–9063.

Yu, Y., Zhang, X. M., Ma, J. P., Liu, Q. K., Wang, P., & Dong, Y. B. (2014). Cu(I)-MOF: naked-eye colorimetric sensor for humidity and formaldehyde in single-crystal-to-single-crystal fashion. *Chemical Communications, 50*, 1444–1446.